

TIP: Text-Driven Image Processing with Semantic and Restoration Instructions

Chenyang Qi^{1,2*} Zhengzhong Tu¹, Keren Ye¹, Mauricio Delbracio¹,
Peyman Milanfar¹, Qifeng Chen², Hossein Talebi¹

¹ Google Research ²HKUST

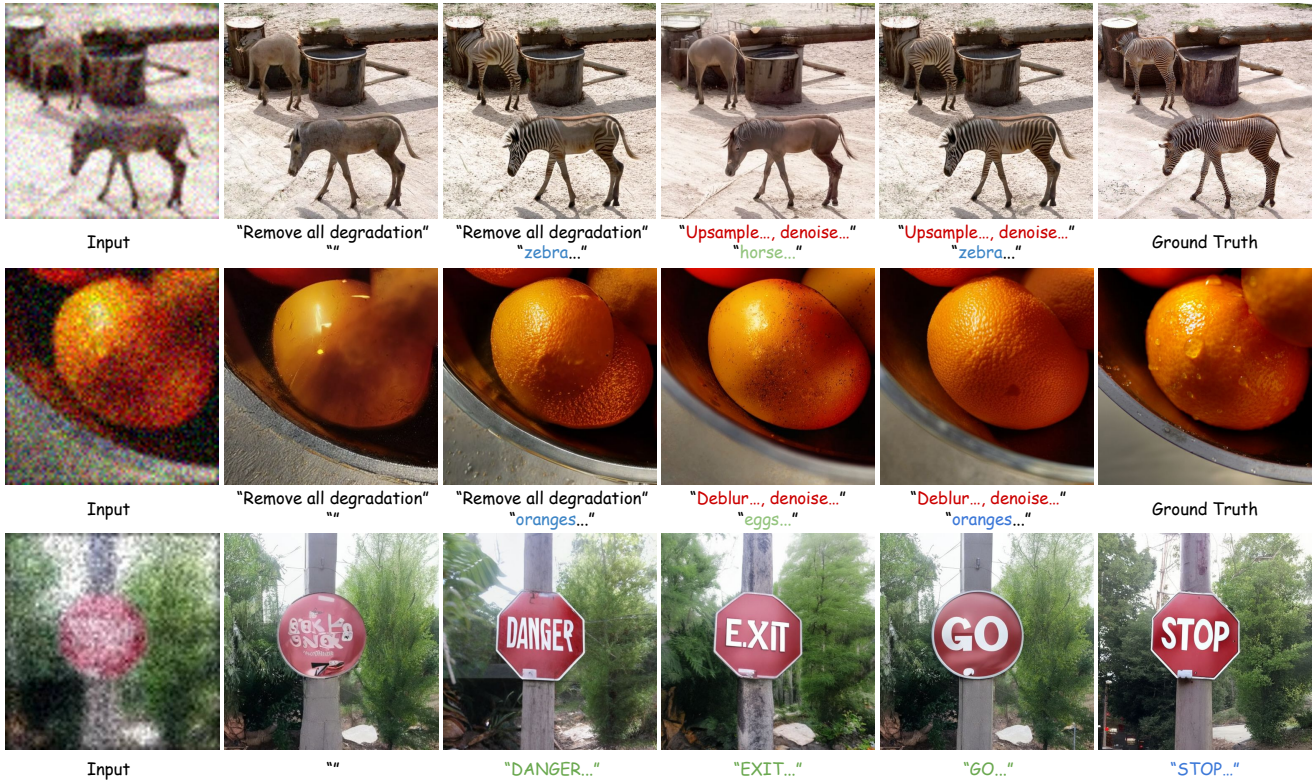


Figure 1. We present **TIP: Text-driven image processing**, a text-based foundation model for all-in-one, instructed image restoration. TIP allows users to flexibly leverage either semantic-level content prompt, or degradation-aware restoration prompt, or both, to obtain their desired enhancement results based on personal preferences. In other words, TIP can be easily prompted to conduct blind restoration, semantic restoration, or task-specific granular treatment. Our framework also enables a new paradigm of **instruction-based image restoration**, providing a reliable evaluation benchmark to facilitate vision-language models for low-level computational photography applications.

Abstract

Text-driven diffusion models have become increasingly popular for various image editing tasks, including inpainting, stylization, and object replacement. However, it still remains an open research problem to adopt this language-vision paradigm for more fine-level image processing tasks, such as denoising, super-resolution, deblurring, and com-

pression artifact removal. In this paper, we develop TIP, a Text-driven Image Processing framework that leverages natural language as a user-friendly interface to control the image restoration process. We consider the capacity of text information in two dimensions. First, we use content-related prompts to enhance the semantic alignment, effectively alleviating identity ambiguity in the restoration outcomes. Second, our approach is the first framework that supports fine-level instruction through language-based quantitative specification of the restoration strength, without the need for explicit task-specific design. In addition,

*This work was done during an internship at Google Research.

we introduce a novel fusion mechanism that augments the existing ControlNet architecture by learning to rescale the generative prior, thereby achieving better restoration fidelity. Our extensive experiments demonstrate the superior restoration performance of TIP compared to the state of the arts, alongside offering the flexibility of text-based control over the restoration effects.

1. Introduction

Image restoration or enhancement aims to recover high-quality, pixel-level details from a degraded image, while preserving as much the original semantic information as possible. Although neural network models [8, 9, 25, 57, 60, 63, 65, 66] have marked significant progress, it still remains challenging to design an effective task-conditioning mechanism instead of building multiple individual models for each task (such as denoise, deblur, compression artifact removal) in practical scenarios. The advancement of text-driven diffusion models [42, 44, 47] has unveiled the potential of natural language as a universal input condition for a broad range of image processing challenges. However, the existing applications of natural language in stylization [32, 38], and inpainting [3, 4, 7, 17, 38, 58] predominantly focus on high-level semantic editing, whereas the uniqueness and challenges for low-level image processing have been less explored.

Natural language text prompts in image restoration can play two crucial roles: alleviating semantic ambiguities and resolving degradation type ambiguities. Firstly, the same degraded image can correspond to different visual objects, leading to ambiguities in content interpretation (e.g., discerning whether the blurred animal in Fig. 1 is a horse or a zebra). Typically, unconditional image-to-image restoration leads to a random or average estimation of the identities, resulting in neither fish nor fowl. Secondly, certain photographic effects that are deliberately introduced for aesthetic purposes, such as *bokeh* with a soft out-of-focus background, can be misconstrued as *blur distortions* by many existing deblurring models, leading to unwanted artifacts or severe hallucinations in the outputs. Although blind restoration methods can produce clean images by either leveraging frozen generative priors [56, 60, 62], or using end-to-end regression [63], they do not consider the aforementioned ambiguities in terms of visual content and degradation types.

In this paper, we introduce **TIP**—a **T**ext-driven **I**mage **P**rocessing framework that provides a user-friendly interface to fully control both the restored image semantics and the enhancement granularity using natural language instructions. TIP takes a degraded image and optional text prompts as inputs (see Figure 1). These text prompts can either specify the restoration types (e.g., “denoise”, “deblur”), or provide semantic descriptions (e.g., “a zebra”, “an orange”).

TIP can be employed in at least three distinct ways:

1. **Blind Restoration:** When instructed with a general prompt “remove all degradations” or empty prompt “”, TIP operates as a blind restoration model (“Ours w/o text” in Tab. 1), without any specific text guidance.
2. **Semantic Restoration:** When provided with a text description of the (desired) visual content, TIP concentrates on restoring the specified identity of the uncertain or ambiguous objects in the degraded image.
3. **Task-Specific Restoration:** Receiving specific restoration type hints (e.g., “deblur...”, “deblur... denoise...”), TIP transforms into a task-specific model (e.g., deblur, denoise, or both). Moreover, it understands the numeric nuances of different degradation parameters in language prompts so that the users can control the restoration strength (e.g., “deblur with sigma 3.0” in Fig. 6).

To train TIP, we first build a synthetic data generation pipeline on a large-scale text-image dataset [6] upon the second-order degradation process proposed in Real-ESRGAN [63]. Additionally, we embed the degradation parameters into the restoration prompts to encode finer-grained degradation information (e.g., “*deblur with sigma 3.5*”). Our approach provides richer degradation-specific information compared to contemporary works [22, 30] which only employ the degradation types (e.g., “gaussian blur”). We then finetune a ControlNet adaptor [71]—which learns a parameter-efficient, parallel branch on top of the latent diffusion models (LDMs) [44]—on a mixture of diverse restoration tasks (see Fig. 1). The semantic text prompts are processed through the LDM backbone, aligning with LDM’s text-to-image pretraining. The degradation text prompts and image-conditioning are implemented in the ControlNet branch, as these aspects are not inherently addressed by the vanilla LDM. We further improve the ControlNet by introducing a new modulation connection that adaptively fuses the degradation condition with the generative prior with only a few extra trainable parameters yet showing impressive performance gain.

Our extensive experiments demonstrate remarkable restoration quality achieved by our proposed TIP method. Moreover, TIP offers additional freedom for both content and restoration prompt engineering. For example, the semantic prompt “*a very large giraffe eating leaves*” helps to resolve the semantic ambiguity in Fig. 2; the degradation prompt “deblur with sigma 3.0” reduces the gaussian blur while maintaining the intentional motion blur in Fig. 3. We also find out that our model learns a continuous latent space of the restoration strength in Fig. 6, even though we do not explicitly fine-tune the CLIP embedding. Our contribution can be summarized as follows:

- We introduce the first unified text-driven image restoration model that supports both semantic prompts and restoration instructions. Our experiments demonstrate

that incorporating semantic prompts and restoration instructions significantly enhances the restoration quality.

- Our proposed paradigm empowers users to fully control the semantic outcome of the restored image using different semantic prompts during test time.
- Our proposed approach provides a mechanism for users to adjust the category and strength of the restoration effect based on their subjective preferences.
- We demonstrate that text can serve as universal guidance control for low-level image processing, eliminating the need for task-specific model design.

2. Related Work

First, we review the literature on image restoration. Our proposed framework aims to address some of the limitations of the existing restoration methods. Next, we compare multiple text-guided diffusion editing methods. Our method is designed to deal with two different text ambiguities concurrently, which is an unprecedented challenge for existing text-driven diffusion methods. Finally, we discuss the parameter-efficient fine-tuning of diffusion models, which further motivates our proposed modulation connection.

Image Restoration is the task of recovering a high-resolution, clean image from a degraded input. Pioneering works in the fields of super-resolution [11, 27], motion and defocus deblurring [1, 55, 67], denoising [68], and JPEG and artifact removal [13, 39] primarily utilize deep neural network architectures to address specific tasks. Later, Transformer-based [25, 57, 65] and adversarial-based [63] formulations were explored, demonstrating state-of-the-art performance with unified model architecture. Recently there has been a focus on exploiting iterative restorations, such as the ones from diffusion models, to generate images with much higher perceptual quality [8, 43, 46, 49, 66]

There have been some recent works attempting to control the enhancement strength of a single model, such as the scaling factor condition in arbitrary super-resolution [61, 64] and noise-level map for image denoising [69]. However, these methods require hand-crafting dedicated architectures for each task, which limits their scalability. In contrast to the task-specific models, other approaches seek to train a single blind model by building a pipeline composed of several classical degradation process, such as BSRGAN [70] and Real-ESRGAN [63].

Text-guided Diffusion Editing Denoising diffusion models are trained to reverse the noising process [20, 51, 52]. Early methods focused on unconditioned generation [10], but recent trends pivot more to conditioned generation, such as image-to-image translation [46, 48] and text-to-image generation [44, 47]. Latent Diffusion [44] is a groundbreaking approach that introduces a versatile framework for improving both training and sampling efficiency, while flexible enough for general conditioning inputs. Subse-

quent works have built upon their pretrained text-to-image checkpoints, and designed customized architectures for different tasks like text-guided image editing. For instance, SDEdit [31] generates content for a new prompt by adding noise to the input image. Attention-based methods [17, 38, 58] show that images can be edited via reweighting and replacing the cross-attention map of different prompts. Aside from the previously mentioned approaches driven by target prompts, instruction-based editing [5, 14] entail modifying a source image based on specific instructions. These textual instructions are typically synthesized using large language models [35, 40].

As CLIP serves as a cornerstone for bridging vision and language, several studies have extensively investigated the representation space of CLIP embeddings [41]. Instead of directly applying CLIP to fundamental discriminative tasks [15, 73], these works either tailor CLIP to specific applications, such as image quality assessment [23, 26], or align image embedding with degradation types in the feature space [22, 30]. To enhance CLIP’s ability to understand numerical information, some works [36, 37] finetune CLIP using contrastive learning on synthetic numerical data, and then incorporate the fine-tuned text embedding into latent diffusion training.

Parameter-Efficient Diffusion Model Finetuning To leverage the powerful generative prior in pretrained diffusion models, parameter-efficient components such as text embedding [12], low-rank approximations of model weights [16, 21], and cross attention layers [24] can be finetuned to personalize the pretrained model. Adaptor-based finetuning paradigms [33, 71] propose to keep the original UNet weights frozen, and add new image or text conditions. This adaptor generates residual features that are subsequently added to the frozen UNet backbone.

3. Method

We introduce a universal approach to combine the above mentioned task-specific, strength-aware, and blind restoration methods within a unified framework (illustrated in Sec. 3.2). We further propose to decouple the learning of content and restoration prompts to better preserve the pretrained prior while injecting new conditions, as unfolded in Sec. 3.3. Sec. 3.4 details our design on how to accurately control the restoration type and strength, as well as our proposed modulation fusion layer that adaptively fuses the restoration features back to the frozen backbone. We start with some preliminaries in the following section.

3.1. Preliminaries

Latent Diffusion Models (LDMs) [44] are probabilistic generative models that learn the underlying data distribution by iteratively removing Gaussian noise in the latent space, which is typically learned using a VAE autoencoder. For-

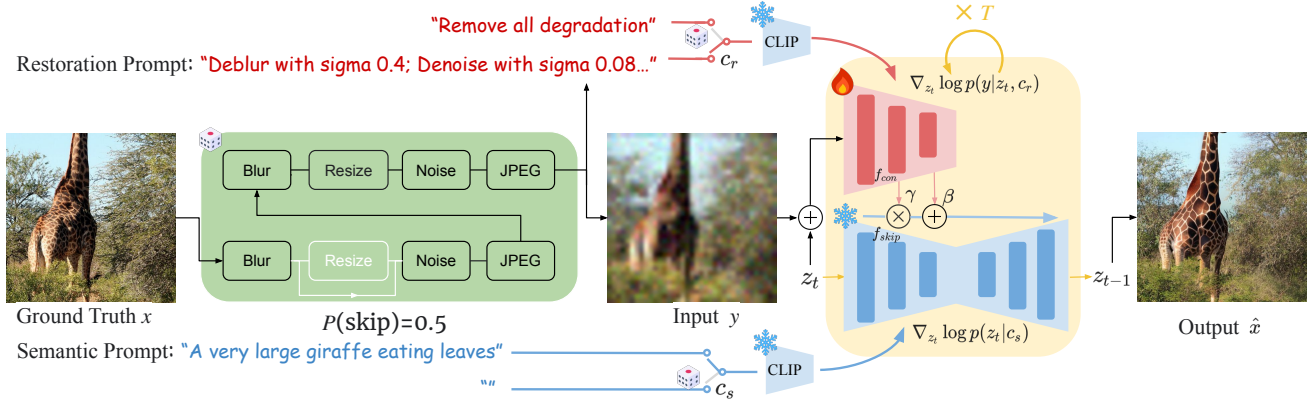


Figure 2. **Framework of TIP.** In the training phase, we begin by synthesizing a degraded version y , of a clean image x . Our degradation synthesis pipeline also creates a restoration prompt c_r , which contains numeric parameters that reflects the intensity of the degradation introduced. Then, we inject the synthetic restoration prompt into a ControlNet adaptor, which uses our proposed modulation fusion blocks (γ, β) to connect with the frozen backbone driven by the semantic prompt c_s . During test time, the users can employ the TIP framework as either a blind restoration model with restoration prompt “Remove all degradation” and empty semantic prompt \emptyset , or manually adjust the restoration c_r and semantic prompts c_s to obtain what they ask for.

mally, the VAE encoder \mathcal{E} compresses an input image x into a compact latent representation $z = \mathcal{E}(x)$, which can be later decoded back to the pixel space using the coupled VAE decoder \mathcal{D} , often learned under an image reconstruction objective: $\mathcal{D}(\mathcal{E}(x)) \approx x$. During training stage, the output of a UNet [45] $\epsilon_\theta(z_t, t, y)$ conditioned on y (such as text, images, etc.) is parameterized [10, 50] to remove Gaussian noise ϵ in the latent space z_t as:

$$\min_{\theta} \mathbb{E}_{(z_0, y) \sim p_{\text{data}}, \epsilon \sim \mathcal{N}(0, I), t} \|\epsilon - \epsilon_\theta(z_t, t, y)\|_2^2, \quad (1)$$

where z_t is a noisy sample of z_0 at sampled timestep t with y representing the conditions. The condition y is randomly dropped out as \emptyset to make the model unconditional.

At test time, deterministic DDIM sampling [51] is utilized to convert a random noise z_T to a clean latent z_0 which is decoded as final result $\mathcal{D}(z_0)$. In each timestep t , classifier-free guidance [10, 19] can be applied to trade-off sample quality and condition alignment:

$$\bar{\epsilon}_\theta(z_t, t, y) = \epsilon_\theta(z_t, t, \emptyset) + w(\epsilon_\theta(z_t, t, y) - \epsilon_\theta(z_t, t, \emptyset)),$$

where w is a scalar to adjust the guidance strength of y . Note that the estimated noise $\bar{\epsilon}_\theta(z_t, t, y)$ is used to update z_t to z_{t-1} , which is a approximation of the distribution gradient score [53] as $\nabla_{z_t} \log p(z_t | y) \propto \bar{\epsilon}_\theta(z_t, t, y)$.

3.2. Text-driven Image Restoration

Based on the LDM framework, we propose a new restoration paradigm—text-driven image restoration. Our method target to restore images (x or z_0) based on conditions $\{y, c_s, c_r\}$. Specifically: y denotes the degraded image condition, c_s is the semantic prompt describing the clean image x (e.g., “a panda is sitting by the bamboo” or “a

panda”), and c_r is the restoration prompt that describes the details of the degradation in terms of both the operation and parameter (e.g., “deblur with sigma 3.0”). We use $y = \text{Deg}(x, c_r)$ to denote the degradation process which turns the clean image x into its degraded counterpart y_i .

The above text-driven image restoration model $p(z_t | \{y, c_s, c_r\})$ can be trained using paired data. We use the text-image dataset [6] so that each clean image x is paired with a semantic prompt c_s (the paired alt-text). Then $y = \text{Deg}(x, c_r)$ is simulated using the synthetic degradation [63] pipeline (Sec. 4.1), yielding the final paired training data $(x \text{ or } z_0, \{y, c_s, c_r\}) \sim p_{\text{data}}$.

Comparing to Blind Restoration Recent existing blind restoration models [29, 48, 60] also leverage diffusion priors to generate high-quality images. However, these methods are prone to hallucinate unwanted, unnatural, or oversharpened textures given that the semantic- and degradation-ambiguities persist everywhere. Fig. 3 provides an example, where the input image is degraded simultaneously with Gaussian blur and motion blur. The fully blind restoration method removes all of the degradation, leaving no way to steer the model to remove only the Gaussian blur while preserving the motion effect for aesthetic purposes. Therefore, having the flexibility to control the restoration behavior and its strength at test time is a crucial requirement. Our text-driven formulation of the problem introduces additional controlling ability using both the semantic content and the restoration instruction. In our TIP design, $c_r = \text{“Remove all degradation”}$ is also a plausible restoration prompt which makes our TIP to be compatible with the blind restoration. Further, our text-driven restoration takes advantages of the pretrained content-aware LDM using the additional semantic prompt c_s , hence able to bet-



Figure 3. **Degradation ambiguities in real-world problems.** By adjusting the restoration prompt, our method can preserve the motion effect that is coupled with the added Gaussian blur, while fully blind restoration models do not provide this level of flexibility.

ter handle semantic ambiguities on the noisy, blurry regions whose visual objects are less recognizable.

3.3. Decoupling Semantic and Restoration Prompts

To effectively learn the latent distribution $p(z_t|\mathbf{y}, \mathbf{c}_s, \mathbf{c}_r)$, we further decouple the conditions $\{\mathbf{y}, \mathbf{c}_s, \mathbf{c}_r\}$ into two groups—one for the text-to-image prior ($\mathbf{c}_s \rightarrow z_t$) already imbued in the pretrained LDM model, and the other for both the image-to-image ($\mathbf{y} \rightarrow z_t$) and restoration-to-image ($\mathbf{c}_r \rightarrow z_t$) that needs to be learnt from the synthetic data. This decoupling strategy prevents catastrophic forgetting in the pretrained diffusion model and enables independent training of the restoration-aware model. The restoration-aware model’s score function [53] is expressed as:

$$\begin{aligned} & \nabla_{z_t} \log p(z_t|\mathbf{y}, \mathbf{c}_s, \mathbf{c}_r) \\ & \approx \underbrace{\nabla_{z_t} \log p(z_t|\mathbf{c}_s)}_{\text{Semantic-aware (frozen)}} + \underbrace{\nabla_{z_t} \log p(\mathbf{y}|z_t, \mathbf{c}_r)}_{\text{Restoration-aware (learnable)}}. \end{aligned} \quad (2)$$

In the above equation, the first part $\nabla_{z_t} \log p(z_t|\mathbf{c}_s)$ aligns with the text-to-image prior inherent in the pretrained LDM. The second term $\nabla_{z_t} \log p(\mathbf{y}|z_t, \mathbf{c}_r)$ approximates the consistency constraint with degraded image \mathbf{y} , meaning the latent image z_t should be inferred by the degraded image \mathbf{y} and the degradation details \mathbf{c}_r . This is somewhat similar to the reverse process of $\mathbf{y} = \text{Deg}(\mathbf{x}_t, \mathbf{c}_r)$ in the pixel space. More derivation is provided in our supplement. Providing degradation information through a restoration text prompt \mathbf{c}_r can largely reduce the uncertainty of estimation $p(\mathbf{y}|z_t, \mathbf{c}_r)$, thereby alleviating the ambiguity of the restoration task and leading to better results that are less prone to hallucinations.

3.4. Learning to Control the Restoration

Inspired by ControlNet [71], we employ an adaptor to model the restoration-aware branch in Eq. (2). First, the pretrained latent diffusion UNet $\epsilon_\theta(z_t, t, \mathbf{c}_s)$ is frozen during training to preserve text-to-image prior $\nabla_{z_t} \log p(z_t|\mathbf{c}_s)$. Secondly, an encoder initialized from pretrained UNet is finetuned to learn the restoration condition $\nabla_{z_t} \log p(\mathbf{y}|z_t, \mathbf{c}_r)$, which takes degradation image \mathbf{y} , current noisy latents z_t and the restoration prompt \mathbf{c}_r as input. The output of encoder is fusion features \mathbf{f}_{con} for frozen

UNet. In this way, the choice of ControlNet implementation follows our decoupling analysis in Eq. (2).

Conditioning on the Degraded Image \mathbf{y} . To feed in the degraded image \mathbf{y} to the ControlNet, we apply downsample layers on \mathbf{y} to make the feature map matching to the shape of the z_t , denoted as $\mathcal{E}'(\mathbf{y})$. \mathcal{E}' is more compact [71] than VAE encoder \mathcal{E} , and its trainable parameters allow model to perceive and adapt to the degraded images from our synthetic data pipeline. Then, we concatenate the downsampled feature map $\mathcal{E}'(\mathbf{y})$ with the latent z_t , and feed them to the ControlNet encoder.

Conditioning on the Restoration Prompt \mathbf{c}_r . Following [44], we first use the vision-language CLIP [41] to infer the text sequence embedding $e_r \in \mathbb{R}^{M \times d}$ for \mathbf{c}_r , where M is the number of tokens, and $d = 768$ is the dimension of the image-text features. Specifically, given a restoration instruction “*deblur with sigma 3.0*”, CLIP first tokenizes it into a sequence of tokens (e.g., “3.0” is tokenized into [“3”, “.”, “0”]) and embeds them into M distinct token embeddings. Then, stacked causal transformer layers [59] are applied on the embedding sequence to contextualize the token embeddings, resulting in e_r . Hence, tokens such as “*deblur*” may arm with the numeric information such as “3”, “.”, and “0”, making it possible for the model to distinguish the semantic difference of strength definition in different restoration tasks. Later, the cross-attention process ensures that the information from e_r is propagated to the ControlNet feature f_{con} . We are aware that [36, 37] finetuned CLIP using contrastive learning, while we found frozen CLIP still works. The reason is that the learnable cross-attention layers can somehow ensemble the observations from frozen CLIP and squeeze useful information from it.

Modulation Fusion Layer The decoupling of learning two branches (Sec. 3.3), despite offering the benefit of effective separation of prior and conditioning, may cause distribution shift in the learned representations between the frozen backbone feature \mathbf{f}_{skip} and ControlNet feature $\mathbf{f}_{control}$. To allow for adaptive alignment of the above features, here we propose a new modulation fusion layer to fuse the multi-scale features from ControlNet to the skip connection features of the frozen backbone:

$$\hat{\mathbf{f}}_{skip} = (1 + \gamma)\mathbf{f}_{skip} + \beta; \quad \gamma, \beta = \mathcal{M}(\mathbf{f}_{con}), \quad (3)$$

where γ, β are the scaling and bias parameters from \mathcal{M} a lightweight 1×1 zero-initialized convolution layer.

4. Experiments

4.1. Text-based Training Data and Benchmarks

Our proposed method opens up an entirely new paradigm of instruction-based image restoration. However, existing image restoration datasets such as DIV2K [2] and Flickr2K [34] do not provide high-quality semantic prompt,

Method	Prompts		Parameterized Degradation with synthesized c_r					Real-ESRGAN Degradation without c_r						
	Sem	Res	FID↓	LPIPS↓	PSNR↑	SSIM↑	CLIP-I↑	CLIP-T↑	FID↓	LPIPS↓	PSNR↑	SSIM↑	CLIP-I↑	CLIP-T↑
SwinIR [25]	✗	✗	43.22	0.423	24.40	0.717	0.856	0.285	48.37	0.449	23.45	0.699	0.842	0.284
StableSR [60]	✗	✗	20.55	0.313	21.03	0.613	0.886	0.298	25.75	0.364	20.42	0.581	0.864	0.298
DiffBIR [29]	✗	✗	17.26	0.302	22.16	0.604	0.912	0.297	19.17	0.330	21.48	0.587	0.898	0.298
ControlNet-SR [71]	✗	✗	13.65	0.222	23.75	0.669	0.938	0.300	16.99	0.269	22.95	0.628	0.924	0.299
Ours w/o text	✗	✗	12.70	0.221	23.84	0.671	0.939	0.299	16.25	0.262	23.15	0.636	0.929	0.300
DiffBIR [29] + SDEdit [31]	✓	✗	19.36	0.362	19.39	0.527	0.891	0.305	17.51	0.375	19.15	0.521	0.887	0.308
DiffBIR [29] + CLIP [41]	✓	✗	18.46	0.365	20.50	0.526	0.896	0.308	20.31	0.374	20.45	0.539	0.885	0.307
ControlNet-SR + CLIP [41]	✓	✗	13.00	0.241	23.18	0.648	0.937	0.307	15.16	0.286	22.45	0.610	0.926	0.308
Ours	✓	✓	11.34	0.219	23.61	0.665	0.943	0.306	14.42	0.262	23.14	0.633	0.935	0.308

Table 1. Quantitative results on the MS-COCO dataset (with c_s) using our parameterized degradation (left) and Real-ESRGAN degradation (right). We also denote the prompt choice at test time. ‘Sem’ stands for semantic prompt; ‘Res’ stands for restoration prompt. The first group of baselines are tested without prompt. The second group are combined with semantic prompt in zero-shot way.

Pipeline	Degradation Process	$p(\text{choose})$	Restoration Prompt
Real-ESRGAN	Blur	1.0	<i>Remove all degradation</i>
	Resize	1.0	
	Noise	1.0	
	JPEG	1.0	
Parameterized	Gaussian Blur	0.5	<i>Deblur with {sigma} or Deblur</i>
	Downsample	0.5	<i>Upsample to {resizing factor} or Upsample</i>
	Gaussian Noise	0.5	<i>Denoise with {sigma} or Denoise</i>
	JPEG	0.5	<i>Dejpeg with quality {jpeg quality} or Dejpeg</i>

Table 2. **Our training degradation** is randomly sampled in these two pipeline with 50% each. (1) Degraded images y synthesized by Real-ESRGAN are paired with the same restoration prompt $c_r = \text{“Remove all degradation”}$ (2) In other 50% iterations, images generated by our **parameterized pipeline** are paired with either a restoration type prompt (e.g., “Deblur”) or a restoration parameter prompt (e.g., “Deblur with sigma 0.3;”).

and Real-ESRGAN degradation is for blind restoration. To address this, we construct a new setting including training data generation and test benchmarks for evaluating text-based restoration models.

Our parameterized degradation pipeline is based on the Real-ESRGAN [63] which contains a large number of degradation types. Since the original full Real-ESRGAN degradation is difficult to be parameterized and represented as user-friendly natural language (e.g., not every one understands “anisotropic plateau blur with beta 2.0”), we choose the 4 most general degradations which are practical for parameterization to support degradation parameter-aware restoration, as shown in Tab. 2. Our parameterized pipeline skips each degradation stage with a 50% probability to increase the diversity of restoration prompts and support single task restoration. The descriptions of the selected degradations are appended following the order of the image degradations to synthesize c_r . In real application, users can control the restoration type and its strength by modifying restoration prompt. As shown in third column of Fig. 3, driven by restoration prompt “Deblur with sigma 3.0”, our framework removes the Gaussian blur, while pre-

serving motion blur. The representation of the restoration strength is also general enough to decouple different tasks in natural language as shown in Fig. 6. More visual results are presented in our supplement.

Training data construction. In the training stage, we sample near 100 million text-image pairs from WebLi [6] and use the alternative text label with highest relevance as the semantic prompt c_s in the framework. We drop out the semantic prompt to empty string \emptyset by a probability of 10% to support semantic-agnostic restoration. We mix the Real-ESRGAN degradation pipeline and our parameterized pipeline by 50% each in training iterations.

Evaluation Setting We randomly choose 3000 pairs of image x and semantic prompt c_s from the MS-COCO [28] validation set. Then, we build two test sets on parameterized and the Real-ESRGAN processes separately. At the left half of Tab. 1, images are sent to the parameterized degradation to form the synthesized degradation image y with restoration prompt c_r . In this setting, we expect “Ours” model to fully utilize the c_s describing the semantic and the c_r describing the degradations. On the right half, the same images are fed to the Real-ESRGAN degradation—so the degradation is aligned with open-sourced checkpoints [25, 29, 60]. Because not every model can utilize both the semantic (c_s) and restoration (c_r) information, Tab. 1 provides a “Prompts” column denoting what information the model relied on. In summary, our constructed benchmarks based on MS-COCO can serve multiple purposes—from fully-blind, content-prompted, to all-prompted restoration.

Evaluation Metrics. We use the generative metric FID [18] and perceptual metric LPIPS [72] for quantitative evaluation of image quality. PSNR, and SSIM are reported for reference. We also evaluate similarity scores in the clip embedding space with ground truth image (CLIP-I) and caption (CLIP-T).

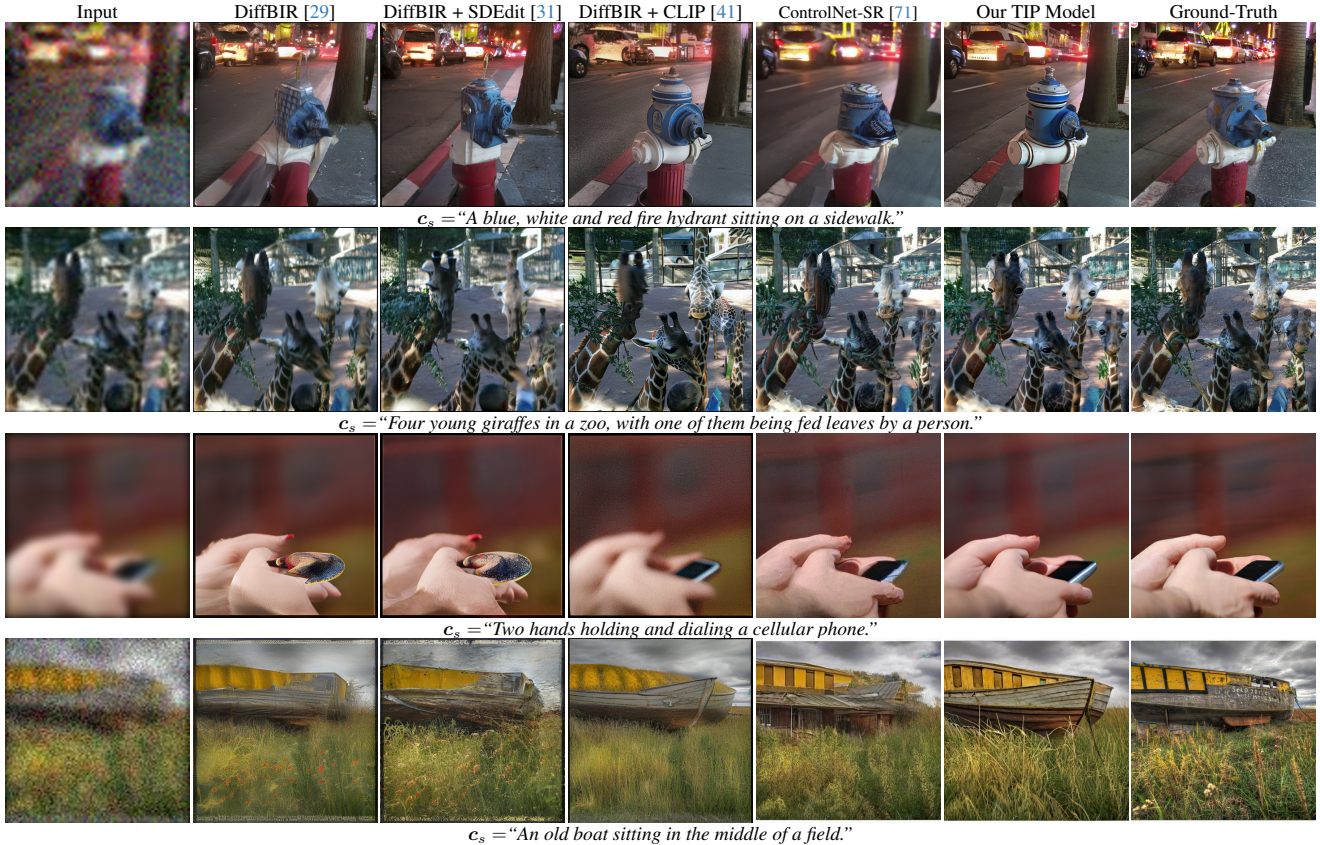


Figure 4. **Visual Comparison with other baselines.** Our method of integrating both the semantic prompt c_s and the restoration prompt c_r outperforms image-to-image restoration (DiffBIR, Retrained ControlNet-SR) and naive zero-shot combination with semantic prompt. It achieves more sharp and clean results while maintaining consistency with the degraded image.

Method	FID↓	LPIPS↓	PSNR↑	SSIM↑	CLIP-I†
DiffBIR [29] (zero-shot)	30.71	0.354	22.01	0.526	0.921
StableSR	24.44	0.311	21.62	0.533	0.928
Ours w/o text (zero-shot)	28.80	0.352	21.68	0.549	0.927
Ours w/o text (finetuned)	22.45	0.321	21.38	0.532	0.932

Table 3. Numerical results on DIV2K testset without any prompt.

4.2. Comparing with baselines

We compare our method with three categories of baselines:

- Open-sourced image restoration checkpoints, including the regression model SwinIR [25] and the latent diffusion models StableSR [60] and DiffBIR [29]
- Combining the state-of-the-art method [29] with the zero-shot post-editing [31] (DiffBIR+SDEdit) or zero-shot injection through CLIP [41] (DiffBIR + CLIP).
- ControlNet-SR [71], an image-to-image model [71] retrained by us for same iteration. It can be driven in zero-shot way as ControlNet-SR+CLIP.

Quantitative Comparison with Baselines is presented in Tab. 1. On the left, we evaluate our full model with the parameterized degradation test set. Since open-sourced baselines are pretrained on Real-ESRGAN degradation, not

perfectly aligned with our parameterized degradation, we also evaluate our full model on MS-COCO with Real-ESRGAN degradation by setting our restoration prompt to “Remove all degradation”. Thanks to our prompts guidance and architecture improvements, our full model achieves best FID, LPIPS, CLIP-Image score, which means better image quality and semantic restoration. “Ours w/o text” is the same checkpoint conditioned on only degradation image and has high pixel-level similarity (the second best PSNR and SSIM) with GT. Although SwinIR has highest PSNR, its visual results are blurry. Although combining semantic prompt in zero-shot way can bring marginal improvement in FID and CLIP similarity with caption, it deteriorates the image restoration capacity and results in worse LPIPS and CLIP-Image. In contrast, semantic prompt guidance improves the CLIP image similarity of our full model. Tab. 3 shows the evaluation results of our model on existing DIV2K test set provided by StableSR. In zero-shot test setting, our model has lower FID and LPIPS than DiffBIR. To fairly compare with StableSR, we finetune our model for 10k iterations on their training set with empty prompt \emptyset . Our finetuned model also outperforms StableSR.



Figure 5. **Test-time semantic prompting.** Our framework restores degraded images guided by flexible semantic prompts, while unrelated background elements and global tones remain aligned with the degraded input conditioning.

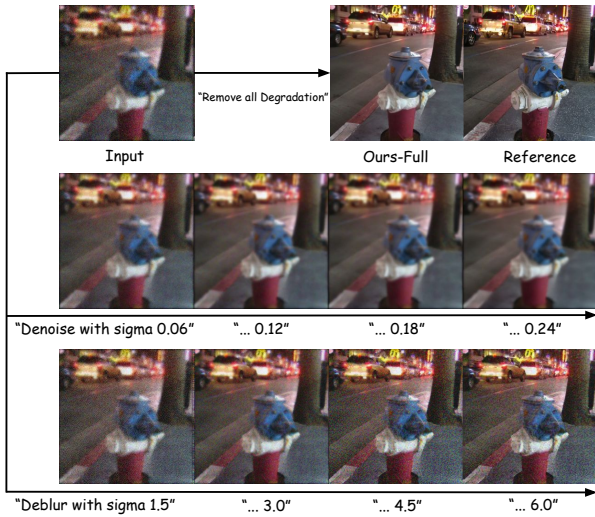


Figure 6. **Prompt space walking visualization for the restoration prompt.** Given the same degraded input (upper left) and empty semantic prompt \emptyset , our method can decouple the restoration direction and strength via only prompting the **quantitative number in natural language**. An interesting finding is that our model learns a continuous range of restoration strength from discrete language tokens.

Qualitative Comparison with Baselines is demonstrated in Fig. 4, where the corresponding semantic prompt is provided below each row. Image-to-image baselines such as DiffBir and the retrained ControlNet-SR can easily generate artifacts (e.g., hydrant in the first row) and blurry images (e.g., hands example in third row) that may look close to an “average” estimation of real images. Besides, naive combination of restoration and semantic prompt in the zero-shot approach results in heavy hallucinations and may fail to preserve the object identity in the input image (e.g., giraffes on the second row). Unlike the existing methods, our full model considers semantic prompt, degradation image and

Method	Sem c_s	Res c_r	FID↓	LPIPS↓	PSNR↑	SSIM↑	CLIP-I↑	CLIP-T↑
ControlNet-SR	✗	✗	13.65	0.222	23.75	0.669	0.938	0.300
ControlNet-SR	✓	✓	12.14	0.223	23.50	0.660	0.940	0.306
Ours	✓	wo param	11.58	0.223	23.61	0.665	0.942	0.305
Ours	✓	✓	11.34	0.219	23.61	0.665	0.943	0.305

Table 4. Ablation of architecture and degradation strength in c_r restoration prompt in both training and test stages, which makes its results more aligned with all conditions.

4.3. Prompting the TIP

Semantic Prompting. Our model can be driven by user-defined semantic prompts at test time. As shown in Fig. 5, the blind restoration with empty string generates ambiguous and unrealistic identity. In contrast, our framework reconstructs sharp and realistic results. The object identity accurately follows the semantic prompt from the user, while the global layout and color tone remain consistent with input.

Restoration Prompting. Users also have the freedom to adjust the degradation types and strengths in the restoration prompts. As shown in Fig. 6, the denoising and deblurring restoration are well decoupled. Using the task-specific prompts, our method can get a clean but blur (second row), or sharp but noisy (third row) result. In addition, our model learns the continuous space of restoration as the result becomes cleaner progressively if we modify the “Denoise with sigma 0.06” to “0.24.”. Beyond purely relying on numerical description, our model “understand” the difference of strength definition for tasks, such as the range difference of denoise sigma and deblur sigma, which makes it promising to be a universal representation for restoration strength control.

4.4. Ablation Study

We conduct several ablations in Tab. 4. Providing both prompts c_s , c_r to “ControlNet-SR” baseline improves the

FID by 1.5. Adding the modulation fusion layer (“Ours”) further improves the generative quality (0.8 for FID) and pixel-level similarity (0.11 dB). Embedding degradation parameters in the restoration prompt, not only enables restoration strength prompting (Fig. 6), but also improves the average image quality as shown by FID and LPIPS. More details are presented in the supplement.

5. Conclusion

We have presented a unified text-driven framework for instructed image processing using semantic and restoration prompts. We design our model in a decoupled way to better preserve the semantic text-to-image generative prior while efficiently learning to control both the restoration direction and its strength. To the best of our knowledge, this is the first framework to support both semantic and parameter-embedded restoration instructions simultaneously, allowing users to flexibly prompt-tune the results up to their expectations. Our extensive experiments have shown that our method significantly outperforms prior works in terms of both quantitative and qualitative results. Our model and evaluation benchmark have established a new paradigm of instruction-based image restoration, paving the way for further multi-modality generative imaging applications.

Acknowledgments. We are grateful to Kelvin Chan and David Salesin for their valuable feedback. We also extend our gratitude to Shlomi Fruchter, Kevin Murphy, Mohammad Babaeizadeh, and Han Zhang for their instrumental contributions in facilitating the initial implementation of the latent diffusion model.

References

- [1] Abdullah Abuolaim, Mauricio Delbracio, Damien Kelly, Michael S Brown, and Peyman Milanfar. Learning to reduce defocus blur by realistically modeling dual-pixel data. In *ICCV*, pages 2289–2298, 2021. 3
- [2] Eirikur Agustsson and Radu Timofte. NTIRE 2017 challenge on single image super-resolution: Dataset and study. In *2017 IEEE Conference on Computer Vision and Pattern Recognition Workshops, CVPR Workshops 2017, Honolulu, HI, USA, July 21-26, 2017*, pages 1122–1131. IEEE Computer Society, 2017. 5
- [3] Omri Avrahami, Dani Lischinski, and Ohad Fried. Blended diffusion for text-driven editing of natural images. In *CVPR*, pages 18208–18218, 2022. 2
- [4] Omri Avrahami, Ohad Fried, and Dani Lischinski. Blended latent diffusion. *ACM Transactions on Graphics*, 2023. 2
- [5] Tim Brooks, Aleksander Holynski, and Alexei A. Efros. Instructpix2pix: Learning to follow image editing instructions. In *CVPR*, 2023. 3
- [6] Xi Chen, Xiao Wang, Soravit Changpinyo, AJ Piergiovanni, Piotr Padlewski, Daniel Salz, Sebastian Alexander Goodman, Adam Grycner, Basil Mustafa, Lucas Beyer, Alexander Kolesnikov, Joan Puigcerver, Nan Ding, Keran Rong, Hassan Akbari, Gaurav Mishra, Linting Xue, Ashish Thapliyal, James Bradbury, Weicheng Kuo, Mojtaba Seyedhosseini, Chao Jia, Burcu Karagol Ayan, Carlos Riquelme, Andreas Steiner, Anelia Angelova, Xiaohua Zhai, Neil Houlsby, and Radu Soricut. Pali: A jointly-scaled multilingual language-image model. In *ICLR*, 2023. 2, 4, 6
- [7] Guillaume Couairon, Jakob Verbeek, Holger Schwenk, and Matthieu Cord. Diffedit: Diffusion-based semantic image editing with mask guidance. *arXiv preprint arXiv:2210.11427*, 2022. 2
- [8] Mauricio Delbracio and Peyman Milanfar. Inversion by direct iteration: An alternative to denoising diffusion for image restoration. *Transactions on Machine Learning Research*, 2023. Featured Certification. 2, 3
- [9] Mauricio Delbracio, Hossein Talebei, and Peyman Milanfar. Projected distribution loss for image enhancement. In *2021 IEEE International Conference on Computational Photography (ICCP)*, pages 1–12. IEEE, 2021. 2
- [10] Prafulla Dhariwal and Alex Nichol. Diffusion models beat gans on image synthesis. *Neural Information Processing Systems*, 2021. 3, 4
- [11] Chao Dong, Chen Change Loy, Kaiming He, and Xiaoou Tang. Image super-resolution using deep convolutional networks. *IEEE Trans. Pattern Anal. Mach. Intell.*, 38(2):295–307, 2016. 3
- [12] Rinon Gal, Yuval Alaluf, Yuval Atzmon, Or Patashnik, Amit H Bermano, Gal Chechik, and Daniel Cohen-Or. An image is worth one word: Personalizing text-to-image generation using textual inversion. In *ICLR*, 2023. 3
- [13] Leonardo Galteri, Lorenzo Seidenari, Marco Bertini, and A. Bimbo. Deep generative adversarial compression artifact removal. In *ICCV*, 2017. 3
- [14] Zigang Geng, Binxin Yang, Tiankai Hang, Chen Li, Shuyang Gu, Ting Zhang, Jianmin Bao, Zheng Zhang, Han Hu, Dong Chen, and Baining Guo. Instructdiffusion: A generalist modeling interface for vision tasks. *CoRR*, abs/2309.03895, 2023. 3
- [15] Xiuye Gu, Tsung-Yi Lin, Weicheng Kuo, and Yin Cui. Open-vocabulary object detection via vision and language knowledge distillation. In *ICLR*, 2021. 3
- [16] Ligong Han, Yinxiao Li, Han Zhang, Peyman Milanfar, Dimitris Metaxas, and Feng Yang. Svdiff: Compact parameter space for diffusion fine-tuning. In *ICCV*, pages 7323–7334, 2023. 3
- [17] Amir Hertz, Ron Mokady, Jay Tenenbaum, Kfir Aberman, Yael Pritch, and Daniel Cohen-or. Prompt-to-prompt image editing with cross-attention control. In *ICLR*, 2023. 2, 3
- [18] Martin Heusel, Hubert Ramsauer, Thomas Unterthiner, Bernhard Nessler, and Sepp Hochreiter. Gans trained by a two time-scale update rule converge to a local nash equilibrium. In *NeurIPS*, 2017. 6
- [19] Jonathan Ho and Tim Salimans. Classifier-free diffusion guidance, 2022. 4
- [20] Jonathan Ho, Ajay Jain, and Pieter Abbeel. Denoising diffusion probabilistic models. *NeurIPS*, 33:6840–6851, 2020. 3

- [21] Edward J Hu, yelong shen, Phillip Wallis, Zeyuan Allen-Zhu, Yuanzhi Li, Shean Wang, Lu Wang, and Weizhu Chen. LoRA: Low-rank adaptation of large language models. In *ICLR*, 2022. 3
- [22] Yitong Jiang, Zhaoyang Zhang, Tianfan Xue, and Jinwei Gu. Autodir: Automatic all-in-one image restoration with latent diffusion. *arXiv preprint arXiv:2310.10123*, 2023. 2, 3
- [23] Junjie Ke, Keren Ye, Jiahui Yu, Yonghui Wu, Peyman Milanfar, and Feng Yang. Vila: Learning image aesthetics from user comments with vision-language pretraining. In *CVPR*, pages 10041–10051, 2023. 3
- [24] Nupur Kumari, Bingliang Zhang, Richard Zhang, Eli Shechtman, and Jun-Yan Zhu. Multi-concept customization of text-to-image diffusion. In *CVPR*, pages 1931–1941, 2023. 3
- [25] Jingyun Liang, Jiezhong Cao, Guolei Sun, Kai Zhang, Luc Van Gool, and Radu Timofte. Swinir: Image restoration using swin transformer. In *Proceedings of ICCV Workshops*, 2021. 2, 3, 6, 7
- [26] Zhixin Liang, Chongyi Li, Shangchen Zhou, Ruicheng Feng, and Chen Change Loy. Iterative prompt learning for unsupervised backlit image enhancement. In *ICCV*, pages 8094–8103, 2023. 3
- [27] Bee Lim, Sanghyun Son, Heewon Kim, Seungjun Nah, and Kyoung Mu Lee. Enhanced deep residual networks for single image super-resolution. In *Proceedings of CVPR Workshops*, 2017. 3
- [28] Tsung-Yi Lin, Michael Maire, Serge Belongie, James Hays, Pietro Perona, Deva Ramanan, Piotr Dollar, and Larry Zitnick. Microsoft coco: Common objects in context. In *ECCV*. ECCV, 2014. 6
- [29] Xinqi Lin, Jingwen He, Ziyang Chen, Zhaoyang Lyu, Ben Fei, Bo Dai, Wanli Ouyang, Yu Qiao, and Chao Dong. Diffbir: Towards blind image restoration with generative diffusion prior. *arXiv preprint arXiv:2308.15070*, 2023. 4, 6, 7, 15
- [30] Ziwei Luo, Fredrik K Gustafsson, Zheng Zhao, Jens Sjölund, and Thomas B Schön. Controlling vision-language models for universal image restoration. *arXiv preprint arXiv:2310.01018*, 2023. 2, 3, 15
- [31] Chenlin Meng, Yutong He, Yang Song, Jiaming Song, Jiajun Wu, Jun-Yan Zhu, and Stefano Ermon. SDEdit: Guided image synthesis and editing with stochastic differential equations. In *ICLR*, 2022. 3, 6, 7, 15
- [32] Ron Mokady, Amir Hertz, Kfir Aberman, Yael Pritch, and Daniel Cohen-Or. Null-text inversion for editing real images using guided diffusion models. In *CVPR*, pages 6038–6047, 2023. 2
- [33] Chong Mou, Xintao Wang, Liangbin Xie, Jian Zhang, Zhonggang Qi, Ying Shan, and Xiaohu Qie. T2i-adapter: Learning adapters to dig out more controllable ability for text-to-image diffusion models. *arXiv preprint arXiv:2302.08453*, 2023. 3
- [34] Seungjun Nah, Radu Timofte, Sungyong Baik, Seokil Hong, Gyeongsik Moon, Sanghyun Son, Kyoung Mu Lee, Xintao Wang, Kelvin C. K. Chan, Ke Yu, Chao Dong, Chen Change Loy, Yuchen Fan, Jiahui Yu, Ding Liu, Thomas S. Huang, Hyeonjun Sim, Munchurl Kim, Dongwon Park, Jisoo Kim, Se Young Chun, Muhammad Haris, Greg Shakhnarovich, Norimichi Ukita, Syed Waqas Zamir, Aditya Arora, Salman H. Khan, Fahad Shahbaz Khan, Ling Shao, Rahul Kumar Gupta, Vishal M. Chudasama, Heena Patel, Kishor P. Upla, Hongfei Fan, Guo Li, Yumei Zhang, Xiang Li, Wenjie Zhang, Qingwen He, Kuldeep Purohit, A. N. Rajagopalan, Jeonghun Kim, Mohammad Tofiqi, Tiantong Guo, and Vishal Monga. NTIRE 2019 challenge on video deblurring: Methods and results. In *IEEE Conference on Computer Vision and Pattern Recognition Workshops, CVPR Workshops 2019, Long Beach, CA, USA, June 16-20, 2019*, pages 1974–1984. Computer Vision Foundation / IEEE, 2019. 5
- [35] OpenAI. Gpt-4 technical report, 2023. 3
- [36] Roni Paiss, Hila Chefer, and Lior Wolf. No token left behind: Explainability-aided image classification and generation. In *ECCV*, 2022. 3, 5
- [37] Roni Paiss, Ariel Ephrat, Omer Tov, Shiran Zada, Inbar Mosseri, Michal Irani, and Tali Dekel. Teaching clip to count to ten. In *ICCV*, 2023. 3, 5
- [38] Gaurav Parmar, Krishna Kumar Singh, Richard Zhang, Yijun Li, Jingwan Lu, and Jun-Yan Zhu. Zero-shot image-to-image translation. In *ACM SIGGRAPH 2023 Conference Proceedings*, pages 1–11, 2023. 2, 3
- [39] Mangal Prakash, Mauricio Delbracio, Peyman Milanfar, and Florian Jug. Interpretable unsupervised diversity denoising and artefact removal. In *ICLR*, 2022. 3
- [40] Alec Radford, Jeffrey Wu, Rewon Child, David Luan, Dario Amodei, Ilya Sutskever, et al. Language models are unsupervised multitask learners. *OpenAI blog*, 1(8):9, 2019. 3
- [41] Alec Radford, Jong Wook Kim, Chris Hallacy, Aditya Ramesh, Gabriel Goh, Sandhini Agarwal, Girish Sastry, Amanda Askell, Pamela Mishkin, Jack Clark, et al. Learning transferable visual models from natural language supervision. In *International conference on machine learning*, pages 8748–8763. PMLR, 2021. 3, 5, 6, 7, 15
- [42] Aditya Ramesh, Prafulla Dhariwal, Alex Nichol, Casey Chu, and Mark Chen. Hierarchical text-conditional image generation with clip latents. *arXiv preprint arXiv:2204.06125*, 2022. 2
- [43] Mengwei Ren, Mauricio Delbracio, Hossein Talebi, Guido Gerig, and Peyman Milanfar. Multiscale structure guided diffusion for image deblurring. In *ICCV*, pages 10721–10733, 2023. 3
- [44] Robin Rombach, Andreas Blattmann, Dominik Lorenz, Patrick Esser, and Björn Ommer. High-resolution image synthesis with latent diffusion models. In *CVPR*, pages 10684–10695, 2022. 2, 3, 5
- [45] Olaf Ronneberger, Philipp Fischer, and Thomas Brox. U-net: Convolutional networks for biomedical image segmentation. In *Medical Image Computing and Computer-Assisted Intervention—MICCAI 2015: 18th International Conference, Munich, Germany, October 5-9, 2015, Proceedings, Part III 18*, pages 234–241. Springer, 2015. 4
- [46] Chitwan Saharia, William Chan, Huiwen Chang, Chris Lee, Jonathan Ho, Tim Salimans, David Fleet, and Mohammad Norouzi. Palette: Image-to-image diffusion models. In *ACM SIGGRAPH 2022 Conference Proceedings*, pages 1–10, 2022. 3

- [47] Chitwan Saharia, William Chan, Saurabh Saxena, Lala Li, Jay Whang, Emily L Denton, Kamyar Ghasemipour, Raphael Gontijo Lopes, Burcu Karagol Ayan, Tim Salimans, et al. Photorealistic text-to-image diffusion models with deep language understanding. *NeurIPS*, 2022. 2, 3
- [48] Chitwan Saharia, Jonathan Ho, William Chan, Tim Salimans, David J Fleet, and Mohammad Norouzi. Image super-resolution via iterative refinement. *IEEE Transactions on Pattern Analysis and Machine Intelligence*, 45(4):4713–4726, 2022. 3, 4
- [49] Chitwan Saharia, Jonathan Ho, William Chan, Tim Salimans, David J Fleet, and Mohammad Norouzi. Image super-resolution via iterative refinement. *IEEE Transactions on Pattern Analysis and Machine Intelligence*, 45(4):4713–4726, 2022. 3
- [50] Tim Salimans and Jonathan Ho. Progressive distillation for fast sampling of diffusion models. In *ICLR*. OpenReview.net, 2022. 4
- [51] Jiaming Song, Chenlin Meng, and Stefano Ermon. Denoising diffusion implicit models. *arXiv preprint arXiv:2010.02502*, 2020. 3, 4
- [52] Yang Song and Stefano Ermon. Generative modeling by estimating gradients of the data distribution. In *NeurIPS*, pages 11895–11907, 2019. 3, 12
- [53] Yang Song, Jascha Sohl-Dickstein, Diederik P Kingma, Abhishek Kumar, Stefano Ermon, and Ben Poole. Score-based generative modeling through stochastic differential equations. In *ICLR*, 2021. 4, 5
- [54] Yang Song, Liyue Shen, Lei Xing, and Stefano Ermon. Solving inverse problems in medical imaging with score-based generative models. In *ICLR*. OpenReview.net, 2022. 12
- [55] Shuochen Su, Mauricio Delbracio, Jue Wang, Guillermo Sapiro, Wolfgang Heidrich, and Oliver Wang. Deep video deblurring for hand-held cameras. In *CVPR*, pages 1279–1288, 2017. 3
- [56] Xuansong Xie Tao Yang, Peiran Ren and Lei Zhang. Gan prior embedded network for blind face restoration in the wild. In *CVPR*, 2021. 2
- [57] Zhengzhong Tu, Hossein Talebi, Han Zhang, Feng Yang, Peyman Milanfar, Alan C. Bovik, and Yinxiao Li. MAXIM: multi-axis MLP for image processing. In *CVPR*, 2022. 2, 3
- [58] Narek Tumanyan, Michal Geyer, Shai Bagon, and Tali Dekel. Plug-and-play diffusion features for text-driven image-to-image translation. In *CVPR*, pages 1921–1930, 2023. 2, 3
- [59] Ashish Vaswani, Noam Shazeer, Niki Parmar, Jakob Uszkoreit, Llion Jones, Aidan N Gomez, Łukasz Kaiser, and Illia Polosukhin. Attention is all you need. *NeurIPS*, 30, 2017. 5
- [60] Jianyi Wang, Zongsheng Yue, Shangchen Zhou, Kelvin CK Chan, and Chen Change Loy. Exploiting diffusion prior for real-world image super-resolution. *arXiv preprint arXiv:2305.07015*, 2023. 2, 4, 6, 7, 12
- [61] Longguang Wang, Yingqian Wang, Zaiping Lin, Jungang Yang, Wei An, and Yulan Guo. Learning a single network for scale-arbitrary super-resolution. In *ICCV*, pages 4801–4810, 2021. 3
- [62] Xintao Wang, Yu Li, Honglun Zhang, and Ying Shan. Towards real-world blind face restoration with generative facial prior. In *CVPR*, 2021. 2
- [63] Xintao Wang, Liangbin Xie, Chao Dong, and Ying Shan. Real-esrgan: Training real-world blind super-resolution with pure synthetic data. In *ICCV*, pages 1905–1914, 2021. 2, 3, 4, 6
- [64] Xiaohang Wang, Xuanhong Chen, Bingbing Ni, Hang Wang, Zhengyan Tong, and Yutian Liu. Deep arbitrary-scale image super-resolution via scale-equivariance pursuit. In *CVPR*, 2023. 3
- [65] Zhendong Wang, Xiaodong Cun, Jianmin Bao, Wengang Zhou, Jianzhuang Liu, and Houqiang Li. Uformer: A general u-shaped transformer for image restoration. In *CVPR*, 2022. 2, 3
- [66] Jay Whang, Mauricio Delbracio, Hossein Talebi, Chitwan Saharia, Alexandros G Dimakis, and Peyman Milanfar. Deblurring via stochastic refinement. In *CVPR*, pages 16293–16303, 2022. 2, 3
- [67] Syed Waqas Zamir, Aditya Arora, Salman Khan, Munawar Hayat, Fahad Shahbaz Khan, Ming-Hsuan Yang, and Ling Shao. Multi-stage progressive image restoration. In *CVPR*, 2021. 3
- [68] Kai Zhang, Wangmeng Zuo, Yunjin Chen, Deyu Meng, and Lei Zhang. Beyond a Gaussian denoiser: Residual learning of deep CNN for image denoising. *IEEE Transactions on Image Processing*, 26(7):3142–3155, 2017. 3
- [69] Kai Zhang, Wangmeng Zuo, and Lei Zhang. Ffdnet: Toward a fast and flexible solution for CNN based image denoising. *IEEE Transactions on Image Processing*, 2018. 3
- [70] Kai Zhang, Jingyun Liang, Luc Van Gool, and Radu Timofte. Designing a practical degradation model for deep blind image super-resolution. In *ICCV*, pages 4791–4800, 2021. 3
- [71] Lvmin Zhang, Anyi Rao, and Maneesh Agrawala. Adding conditional control to text-to-image diffusion models. In *ICCV*, 2023. 2, 3, 5, 6, 7
- [72] Richard Zhang, Phillip Isola, Alexei A Efros, Eli Shechtman, and Oliver Wang. The unreasonable effectiveness of deep features as a perceptual metric. In *CVPR*, 2018. 6
- [73] Renrui Zhang, Rongyao Fang, Peng Gao, Wei Zhang, Kunchang Li, Jifeng Dai, Yu Qiao, and Hongsheng Li. Tip-adapter: Training-free clip-adapter for better vision-language modeling. In *ECCV*, 2022. 3

A. Implementation Details

A.1. Derivation Details in Equation 2

We propose to compute the distribution of latents $p(\mathbf{z}_t|\mathbf{y}, \mathbf{c}_s, \mathbf{c}_r)$ conditioned on degraded image \mathbf{y} , semantic prompt \mathbf{c}_s and restoration prompt \mathbf{c}_r . Using the Bayes’ decomposition similar to score-based inverse problem [52, 54], we have

$$p(\mathbf{z}_t|\mathbf{y}, \mathbf{c}_s, \mathbf{c}_r) = p(\mathbf{z}_t, \mathbf{y}, \mathbf{c}_s, \mathbf{c}_r)/p(\mathbf{y}, \mathbf{c}_s, \mathbf{c}_r). \quad (4)$$

Then, we compute gradients with respect to \mathbf{z}_t , and remove the gradients of input condition $\nabla_{\mathbf{z}_t} \log p(\mathbf{y}, \mathbf{c}_s, \mathbf{c}_r) = 0$ as:

$$\begin{aligned} \nabla_{\mathbf{z}_t} \log p(\mathbf{z}_t|\mathbf{y}, \mathbf{c}_s, \mathbf{c}_r) \\ = \nabla_{\mathbf{z}_t} \log p(\mathbf{z}_t, \mathbf{y}, \mathbf{c}_s, \mathbf{c}_r) \end{aligned} \quad (5)$$

$$= \nabla_{\mathbf{z}_t} \log [p(\mathbf{c}_s) \cdot p(\mathbf{z}_t|\mathbf{c}_s) \cdot p(\mathbf{y}, \mathbf{c}_r|\mathbf{c}_s, \mathbf{z}_t)] \quad (6)$$

$$= \nabla_{\mathbf{z}_t} \log [p(\mathbf{z}_t|\mathbf{c}_s) \cdot p(\mathbf{y}, \mathbf{c}_r|\mathbf{c}_s, \mathbf{z}_t)] \quad (7)$$

$$= \nabla_{\mathbf{z}_t} \log p(\mathbf{z}_t|\mathbf{c}_s) + \nabla_{\mathbf{z}_t} \log p(\mathbf{y}, \mathbf{c}_r|\mathbf{c}_s, \mathbf{z}_t) \quad (8)$$

We assume \mathbf{y} is generated through a degradation pipeline as $\mathbf{y} = \text{Deg}(\mathbf{x}, \mathbf{c}_r)$, thus it is independent of \mathbf{c}_s with \mathbf{x} and \mathbf{c}_r provided as condition. Removing redundant \mathbf{c}_s condition, the second term in the last equation can be approximated as:

$$\begin{aligned} \nabla_{\mathbf{z}_t} \log p(\mathbf{y}, \mathbf{c}_r|\mathbf{c}_s, \mathbf{z}_t) \\ \approx \nabla_{\mathbf{z}_t} \log p(\mathbf{y}, \mathbf{c}_r|\mathbf{z}_t) \end{aligned} \quad (9)$$

$$= \nabla_{\mathbf{z}_t} \log p(\mathbf{c}_r|\mathbf{z}_t) + \nabla_{\mathbf{z}_t} \log p(\mathbf{y}|\mathbf{z}_t, \mathbf{c}_r) \quad (10)$$

$$= \nabla_{\mathbf{z}_t} \log p(\mathbf{y}|\mathbf{z}_t, \mathbf{c}_r) \quad (11)$$

In summary of the above equations, we derive the Equation 2 in the main manuscript

$$\begin{aligned} \nabla_{\mathbf{z}_t} \log p(\mathbf{z}_t|\mathbf{y}, \mathbf{c}_s, \mathbf{c}_r) \\ \approx \underbrace{\nabla_{\mathbf{z}_t} \log p(\mathbf{z}_t|\mathbf{c}_s)}_{\text{Semantic-aware (froze)}} + \underbrace{\nabla_{\mathbf{z}_t} \log p(\mathbf{y}|\mathbf{z}_t, \mathbf{c}_r)}_{\text{Restoration-aware (learnable)}}, \end{aligned} \quad (12)$$

where $\nabla_{\mathbf{z}_t} \log p(\mathbf{y}|\mathbf{z}_t, \mathbf{c}_r)$ is synthesized using stochastic degradation pipeline $\mathbf{y} = \text{Deg}(\mathbf{x}, \mathbf{c}_r)$ to train our ControlNet.

A.2. Pseudo Code for Degradation Synthesis

To support the learning of restoration-aware term $\nabla_{\mathbf{z}_t} \log p(\mathbf{y}|\mathbf{z}_t, \mathbf{c}_r)$, we synthesized the degradation image \mathbf{y} using clean image \mathbf{x} with the algorithm presented in Algorithm 1. First, we randomly choose one from Real-ESRGAN pipeline and our parameterized degradation. Then the degraded image from Real-ESRGAN pipeline is paired with restoration prompt $\mathbf{c}_r = \text{“Remove all degradation”}$. In our parameterized degradation, all processes are paired with restoration prompts \mathbf{c}_{rp} listed in Table 2 of the main manuscript (e.g., *Deblur with sigma 3.0*).

Algorithm 1 TIP Degradation Pipeline in Training

Inputs: \mathbf{x} : Clean image

Outputs: \mathbf{y} : Degraded image; \mathbf{c}_r : Restoration prompt

type \leftarrow RANDCHOICE(Real-ESRGAN, Param)

if type = Real-ESRGAN **then**

 // Real-ESRGAN degradation

$\mathbf{y} \leftarrow \mathbf{x}$

 Deg \leftarrow RANDOM(Real-ESRGAN-Degradation)

for PROCESS in Deg **do**:

$\mathbf{y} \leftarrow$ PROCESS(\mathbf{y})

end for

$\mathbf{c}_r \leftarrow$ “Remove all degradation”

else

 // Parameterized degradation

$\mathbf{c}_r \leftarrow \emptyset$

$\mathbf{y} \leftarrow \mathbf{x}$

 Deg \leftarrow RANDOM(Parameterized-Degradation)

for PROCESS, \mathbf{c}_{rp} in Deg **do**:

$\mathbf{y} \leftarrow$ PROCESS($\mathbf{y}, \mathbf{c}_{rp}$)

$\mathbf{c}_r \leftarrow$ CONCAT($\mathbf{c}_r, \mathbf{c}_{rp}$)

end for

end if

return \mathbf{y}, \mathbf{c}_r

B. More Ablation Study

Tab. 5 provides more comprehensive ablations of text prompts by providing different information to our image-to-image baseline. Semantic prompts significantly improve image quality as shown in better FID and CLIP-Image, but reduce the similarity with ground truth image. Restoration types and parameters embedded in the restoration prompts both improve image quality and fidelity. Tab. 6 presents a comparison of our skip feature modulation f_{skip} with that in StableSR [60] which modulates both skip feature f_{skip} from encoder and upsampling feature f_{up} from decoder. We observe that modulating f_{up} does not bring obvious improvements. One possible reason is that γ and β of the middle layer adapts to the feature in the upsampling layers.

C. More Semantic Prompting

As shown in the Fig. 7, our framework supports semantic descriptions for restoring multiple objects.

D. More Restoration Prompting

Fig. 8 shows the application of restoration prompt on out-of-domain data, including Midjourney image and real-world cartoon. Since these images are not in our training data domain, a blind enhancement with prompt “Remove all degradation” can not achieve satisfying results. Utiliz-



Figure 7. More semantic prompting for images with multiple objects.

Method	Sem	Res Type	Res Param	FID↓	LPIPS↓	PSNR↑	SSIM↑	CLIP _{im} ↑	CLIP _{tx} ↑
Ours	✗	✗	✗	13.60	0.221	23.65	0.664	0.939	0.300
Ours	✓	✗	✗	11.71	0.226	23.55	0.663	0.941	0.305
Ours	✓	✓	✗	11.58	0.223	23.61	0.665	0.942	0.305
Ours	✓	✓	✓	11.34	0.219	23.61	0.665	0.943	0.306

Table 5. Ablation of prompts provided during both training and testing. We use an image-to-image model with our modulation fusion layer as our baseline. Providing semantic prompts significantly increases the image quality (1.9 lower FID) and semantic similarity (0.002 CLIP-Image), but results in worse pixel-level similarity. In contrast, degradation type information embedded in restoration prompts improves both pixel-level fidelity and image quality. Utilizing degradation parameters in the restoration instructions further improves these metrics.

Method	Modulate f_{skip}	Modulate f_{up}	Relative Param	FID↓	LPIPS↓
Ours w/ prompts	✗	✗	1	12.14	0.223
Ours w/ prompts	✓	✓	1.06	11.21	0.219
Ours w/ prompts	✓	✗	1.03	11.34	0.219

Table 6. Ablation of the architecture. Modulating the skip feature f_{skip} improves the fidelity of the restored image with 3% extra parameters in the adaptor, while further modulating the backbone features f_{up} does not bring obvious advantage.

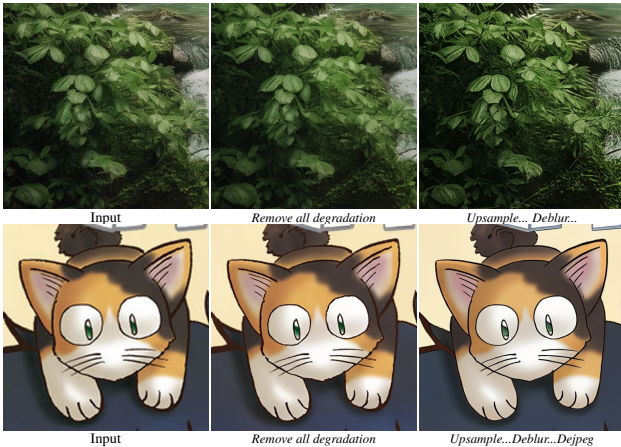


Figure 8. Restoration prompting for out-of-domain images.

ing restoration prompting (e.g., “Upsample to 6.0x; Deblur with sigma 2.9;”) can successfully guide our model to improve the details and color tones of the Midjourney image. In the second row, a manually designed restoration prompt also reduces the jagged effect to smooth the lines in the cartoon image.

To study whether the model follows restoration instruc-

tions, a dense walking of restoration prompt is presented in Fig. 9. From left to right, we increase the strength of denoising in the restoration prompt. From top to the bottom, the strength of deblurring gets larger. The results demonstrates that our restoration framework refines the degraded image continuously following the restoration prompts

E. More Visual Comparison

More visual comparisons with baselines are provided in Fig. 10.

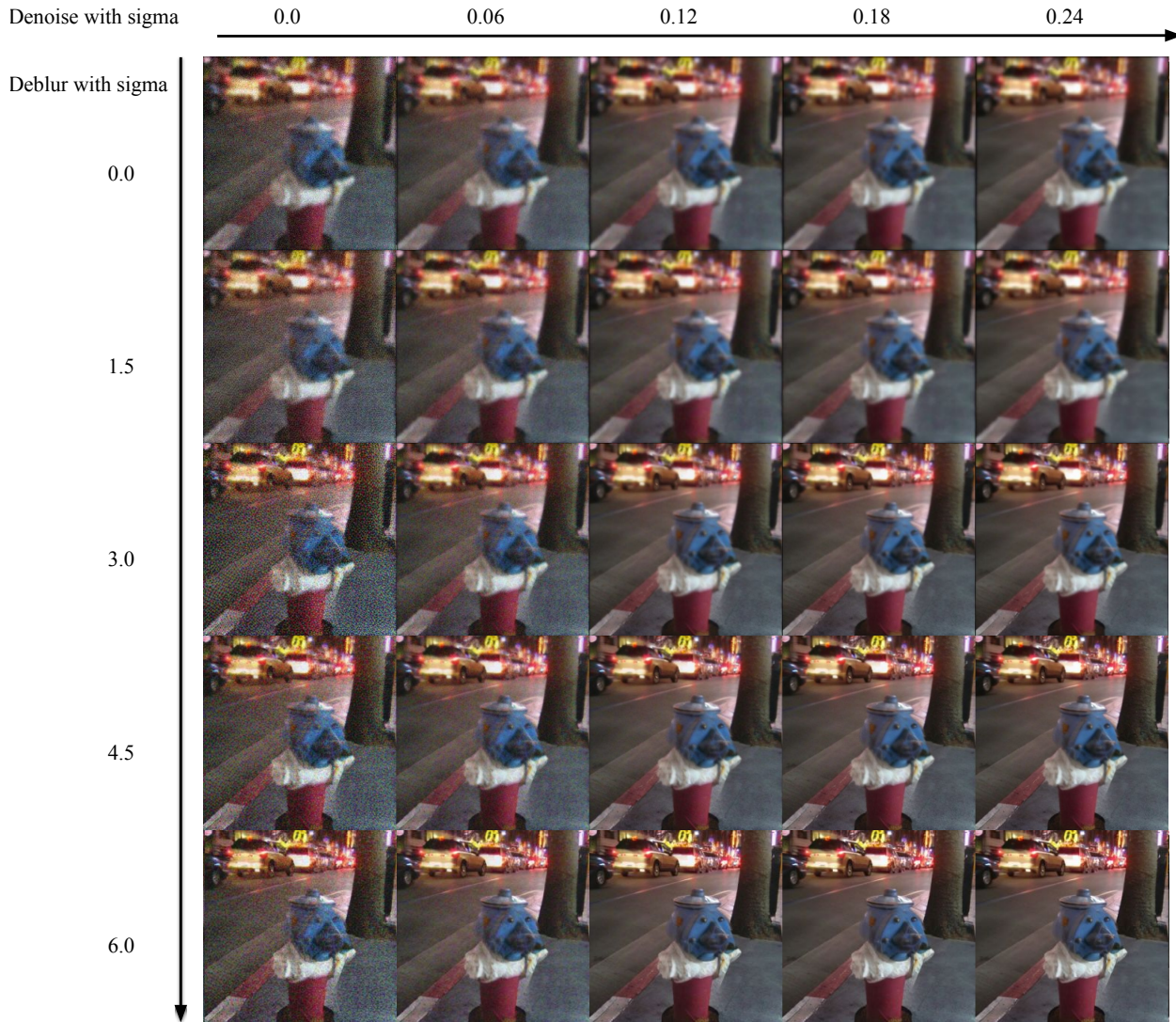


Figure 9. **Prompt space walking visualization for the restoration prompt.** Given the same degraded input (upper left) and empty semantic prompt \emptyset , our method can decouple the restoration direction and strength via only prompting the **quantitative number in natural language**. An interesting finding is that our model learns a continuous range of restoration strength from discrete language tokens.

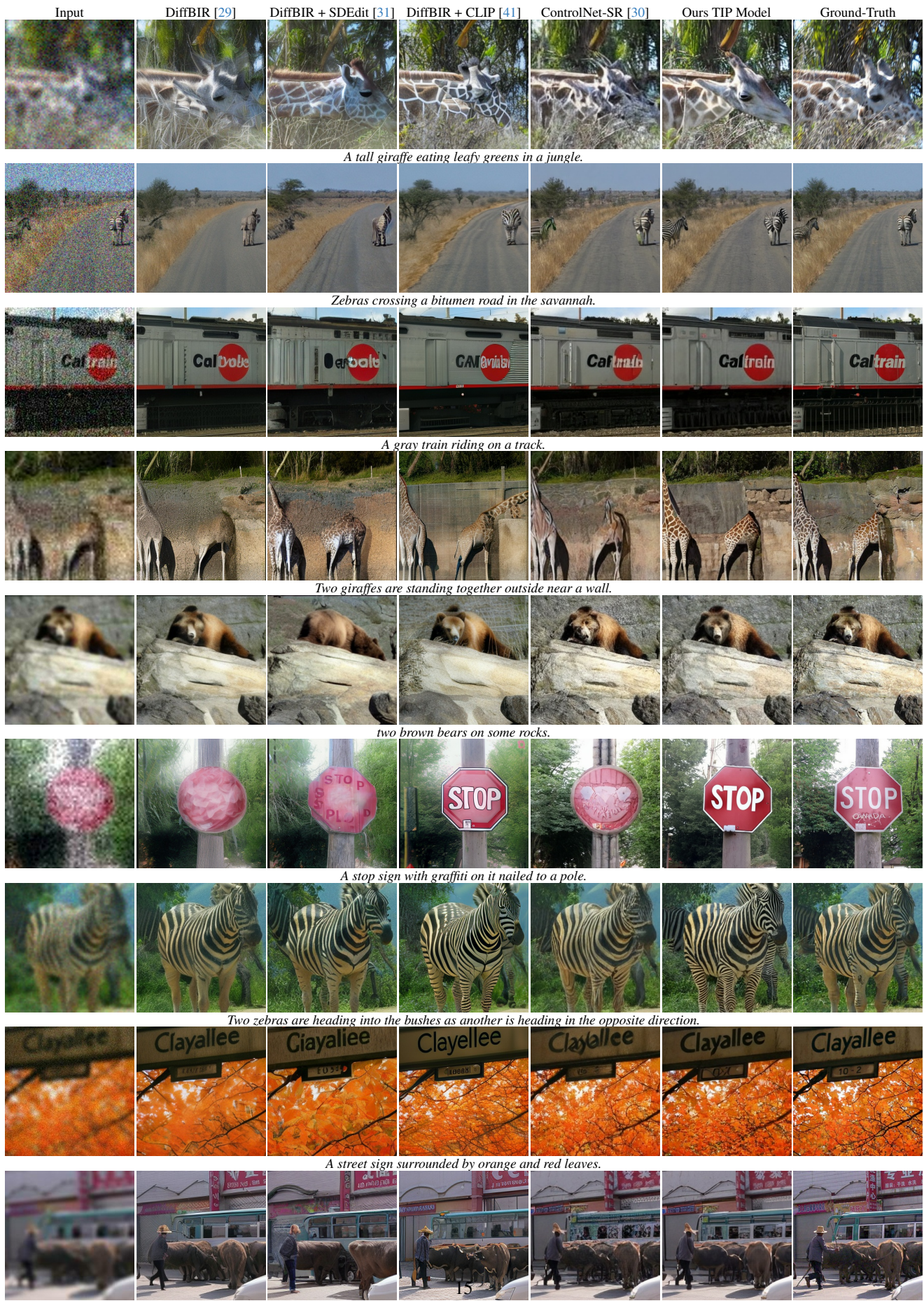


Figure 10. Main visual comparison with baselines. (Zoom in for details)